Brain monoamine vesicular transport disease caused by homozygous *SLC18A2* variants: a study in 42 affected individuals

Ken Saida[1, 60], Reza Maroofian[2, 60], Toru Sengoku[3], Tadahiro Mitani[4], Alistair T Pagnamenta[5], Dana Marafi[4, 6], Maha S Zaki[7], Thomas J O'Brien[8, 9], Ehsan Ghayoor Karimiani[10, 11], Rauan Kaiyrzhanov[2], Marina Takizawa[1], Sachiko Ohori[1], Huey Yin Leong[12], Gulsen Akay[4], Hamid Galehdari[13], Mina Zamani[13], Ratna Romy[10], Christopher J Carroll[10], Mehran Beiraghi Toosi[14, 15], Farah Ashrafzadeh[14], Shima Imannezhad[16], Hadis Malek[17], Najmeh Ahangari[17], Hoda Tomoum[18], Vykuntaraju K Gowda[19], Varunvenkat M Srinivasan[19], David Murphy[20], Natalia Dominik[2], Hasnaa M Elbendary[7], Karima Rafat[7], Sanem Yilmaz[21], Seda Kanmaz[21], Mine Serin[21], Deepa Krishnakumar[22], Alice Gardham[22], Anna Maw[23], Tekki Sreenivasa Rao[24], Sarah Alsubhi[25], Myriam Srour[25, 26], Daniela Buhas[27, 28], Tamison Jewett[29], Rachel E Goldberg[29], Hanan Shamseldin[30], Eirik Frengen[31], Doriana Misceo[31], Petter Strømme[32], José Ricardo Magliocco Ceroni[33], Chong Ae Kim[33], Gozde Yesil[34], Esma Sengenc[35], Serhat Guler[36], Mariam Hull[37], Mered Parnes[37], Dilek Aktas[38], Banu Anlar[39], Yavuz Bayram[40, 41], Davut Pehlivan[4, 37, 42], Jennifer E Posey[4], Shahryar Alavi[43], Seyed Ali Madani Manshadi[44], Hamad Alzaidan[45], Mohammad Al-Owain[45], Lama Alabdi[30], Ferdous Abdulwahab[30], Futoshi Sekiguchi[1], Kohei Hamanaka[1], Atsushi Fujita[1], Yuri Uchiyama[1, 46], Takeshi Mizuguchi[1], Satoko Miyatake[1,47], Noriko Miyake[1, 48], Reem M Elshafie[49], Kamran Salayev[50], Ulviyya Guliyeva[51], Fowzan S Alkuraya[30,52], Joseph G Gleeson[53, 54], Kristin G Monaghan[55], Katherine G Langley[55], Hui Yang[55], Mahsa Motavaf[56], Saeid Safari[56], Mozhgan Alipour[56, 57], Kazuhiro Ogata[3], André EX Brown[8, 9], James R Lupski[4, 37, 58, 59], Henry Houlden[2, 61], and Naomichi Matsumoto[1, 61]

Affiliations

[1]Department of Human Genetics, Yokohama City University Graduate School of Medicine, Yokohama, Japan, [2]Department of Neuromuscular Disorders, UCL Queen Square Institute of Neurology, University College London, London, UK, [3]Department of Biochemistry, Yokohama City University Graduate School of Medicine, Yokohama, Japan, [4]Department of Molecular and Human Genetics, Baylor College of Medicine, Houston, TX, USA, [5]NIHR Oxford BRC, Wellcome Centre for Human Genetics, University of Oxford, Oxford, UK, [6]Department of Pediatrics, Faculty of Medicine, Kuwait University, Safat, Kuwait, [7]Department of Clinical Genetics, Human Genetics and Genome Research Institute, National Research Centre, Cairo, Egypt, [8]MRC London Institute of Medical Sciences, London, UK, [9]Faculty of Medicine, Institute of Clinical

Sciences, Imperial College London, London, UK, [10]Molecular and Clinical Sciences Research Institute, St. George's, University of London, London, UK, [11]Innovative Medical Research Center, Mashhad branch, Islamic Azad University, Mashhad, Iran, [12]Genetics Department, Hospital Kuala Lumpur, Kuala Lumpur, Malaysia, [13]Department of Biology, Faculty of Science, Shahid Chamran University of Ahvaz, Ahvaz, Iran, [14]Department of Pediatrics, Faculty of Medicine, Mashhad University of Medical Sciences, Mashhad, Iran, [15]Neuroscience Research Center, Mashhad University of Medical Sciences, Mashhad, Iran, [16]Department of Pediatric Neurology, Faculty of Medicine, Mashhad University of Medical Sciences, Mashhad, Iran, [17]Department of Medical Genetics, Next Generation Genetic Polyclinic, Mashhad, Iran, [18]Department of Pediatrics, Ain Shams University, Cairo, Egypt, [19]Department of Pediatric Neurology, Indira Gandhi Institute of Child Health, Bangalore, India, [20]Department of Clinical and Movement Neurosciences, UCL Queen Square Institute of Neurology, University College London, UK, [21]Division of Pediatric Neurology, Department of Pediatrics, Ege University Faculty of Medicine, Izmir, Turkey, [22]North West Thames Regional Genetics Service, Northwick Park Hospital, London, UK, [23]Depatment of Paediatric Neurology, Cambridge University Hospitals NHS Foundation Trust, Cambridge, UK, [24]Deparment of Paediatrics, Luton and Dunstable University Hospital, Luton, UK, [25]Division of Pediatric Neurology, Departments of Pediatrics, McGill University, Montreal, QC, Canada, [26]McGill University Health Center (MUHC) Research Institute, QC, Montreal, Canada, [27]Division of Medical Genetics, Department of Specialized Medicine, McGill University Health Center (MUHC), Montreal, QC, Canada, [28]Department of Human Genetics, McGill University, Montreal, QC, Canada, [29]Department of Pediatrics, Section on Medical Genetics, Wake Forest University School of Medicine, Winston-Salem, NC, USA, [30]Department of Translational Genomics, Center for Genomic Medicine, King Faisal Specialist Hospital and Research Center, Riyadh, Saudi Arabia, [31]Department of Medical Genetics, Oslo University Hospital and University of Oslo, Oslo, Norway, [32]Division of Pediatric and Adolescent Medicine, Oslo University Hospital and University of Oslo, Oslo, Norway, [33]Genetic Unit, Instituto da Crianca, Faculdade de Medicina, Universidade de Sao Paulo, Sao Paulo, Brazil, [34]Istanbul University, Istanbul Medical Faculty, Department of Medical Genetics, Istanbul, Turkey, [35]Bezmialem Vakif University, Medical Faculty, Department of Child Neurology, Istanbul, Turkey, [36]Istanbul University, Cerrahpasa Medical Faculty, Department of Child Neurology, Istanbul, Turkey, [37]Texas Children's Hospital, Houston, TX, USA, [38]Damagen Genetic Diagnostic Center, Ankara, Turkey, [39]Hacettepe University Faculty of Medicine, Department of Pediatric Neurology, Ankara, Turkey, [40]Division of

Genomic Diagnostics, Department of Pathology and Laboratory Medicine, Children's Hospital of Philadelphia, Philadelphia, PA, USA, [41]Perelman School of Medicine, University of Pennsylvania, Philadelphia, PA, USA, [42]Section of Pediatric Neurology and Developmental Neuroscience, Department of Pediatrics, Baylor College of Medicine, Houston, TX, USA, [43]Department of Cell and Molecular Biology and Microbiology, Faculty of Biological Science and Technology, University of Isfahan, Isfahan, Iran, [44]Meybod Genetic Research Center, Meybod, Yazd, Iran, [45]Department of Medical Genomics, Centre for Genomic Medicine, King Faisal Specialist Hospital and Research Center, Riyadh, Saudi Arabia, [46]Department of Rare Disease Genomics, Yokohama City University Hospital, Yokohama, Japan, [47]Clinical Genetics Department, Yokohama City University Hospital, Yokohama, Japan, [48]Department of Human Genetics, Research Institute, National Center for Global Health and Medicine, Tokyo, Japan, [49]Kuwait Medical Genetic Centre, Ministry of Health, Kuwait, [50]Department of Neurology, Azerbaijan Medical University, Baku, Azerbaijan, [51]MediClub Hospital, Baku, Azerbaijan, [52]Department of Anatomy and Cell Biology, College of Medicine, Alfaisal University, Riyadh, Saudi Arabia, [53]Department of Neurosciences, University of California, San Diego, CA, USA, [54]Rady Children's Institute for Genomic Medicine, San Diego, CA, USA, [55]GeneDx, Gaithersburg, MD, USA., [56]Functional Neurosurgery Research Center, Shohada Tajrish Comprehensive Neurosurgical Center of Excellence, Shahid Beheshti University of Medical Sciences, Tehran, Iran, [57]Department of Biophysics, Faculty of Biological Sciences, Tarbiat Modares University, Tehran, Iran, [58]Human Genome Sequencing Center, Baylor College of Medicine, Houston, TX, USA, [59]Department of Pediatrics, Baylor College of Medicine, Houston, TX, USA, [60]These authors contributed equally: Ken Saida, Reza Maroofian. [61]These authors contributed equally: Henry Houlden, Naomichi Matsumoto.

Correspondence: Naomichi Matsumoto
Department of Human Genetics, Graduate School of Medicine, Yokohama City University, 3-9 Fukuura, Kanazawa−ku, Yokohama 236-0004, Japan
E-mail: naomat@yokohama-cu.ac.jp

Abstract

Purpose: Brain monoamine vesicular transport disease is an infantile-onset movement disorder that mimics cerebral palsy. In 2013, the homozygous *SLC18A2* variant, p.Pro387Leu, was first reported as a cause of this rare disorder, and dopamine agonists were efficient for treating affected individuals from one large family. To date, only six variants have been reported. Here, we evaluated genotype–phenotype correlations in individuals with biallelic *SLC18A2* variants.

Methods: Forty-two affected individuals with homozygous *SLC18A2* variant alleles were identified. We evaluated genotype–phenotype correlations and the missense variants in the affected individuals, based on the structural modeling of rat vesicular monoamine transporter type 2 encoded by *Slc18a2*, with cytoplasm- and lumen-facing conformations. A *Caenorhabditis elegans* model was created for functional studies.

Results: Nineteen homozygous *SLC18A2* variants, including three recurrent variants, were identified using exome sequencing. The affected individuals typically showed global developmental delay, hypotonia, dystonia, oculogyric crisis, and autonomic nervous involvement (temperature dysregulation/sweating, hypersalivation, and gastrointestinal dysmotility). Among the 58 affected individuals described to date, 16 (28%) died before the age of 13 years. Nine of the 17 patients with p.Pro237His died,

whereas all 14 patients with p.Pro387Leu survived. Although a dopamine receptor agonist mildly improved the disease symptoms in 17 of 21 patients (81%), some affected individuals with p.Ile43Phe and p.Pro387Leu showed milder phenotypes and, presented prolonged survival, even without treatment. The *C. elegans* model showed behavioral abnormalities.

Conclusions: These data expand the phenotypic and genotypic spectra of *SLC18A2*-related disorders.

Keywords: solute carrier family 18 member A2, brain vesicular monoamine transporter type 2, brain monoamine vesicular transport disease, dopamine agonist, Parkinsonism, dystonia

Abbreviations: SLC18A2: solute carrier family 18 member A2; VMAT2: brain vesicular monoamine transporter type 2; rVMAT2: rat VMAT2; TM1: transmembrane helix 1

INTRODUCTION

Monoamine neurotransmitter disorders are rare heterogeneous neurological disorders

mostly presenting during early life.[1,2] Many neurotransmitter disorders resemble the phenotypes of other neurological disorders (e.g., cerebral palsy and hypoxic ischemic encephalopathy) and are thus sometimes misdiagnosed.[3] When dyskinetic movements occur in combination with autonomic dysregulation, there is a possibility of a neurotransmitter disease, and hence, genetic diagnosis should be considered. Biallelic loss-of-function (LoF) variants in *SLC6A3* (MIM*126455), which encodes a dopamine transporter, cause infantile-onset Parkinsonism-dystonia 1 (PKDYS1; MIM# 613135), known as dopamine transporter deficiency syndrome (DATS), the first monoamine transportopathy to be described.[4,5] Brain vesicular monoamine transporter type 2 (VMAT2), encoded by the solute carrier family 18 member A2 gene (*SLC18A2*, MIM*193001), facilitates dopamine and serotonin loading into synaptic vesicles for their transport to the cell membrane and the subsequent release.[6] Biallelic dysfunction of *SLC18A2* causes brain monoamine vesicular transport disease (infantile-onset Parkinsonism-dystonia 2 [PKDYS2]; MIM# 618049).[7]

Heterozygous *Slc18a2*-knockout mice express half the amount of VMAT2 in the brain compared with that in the wild-type mice, and homozygous knockout mice do not express VMAT2 and have poor postnatal viability.[6,8] A homozygous *SLC18A2* variant (c.1160C>T p.Pro387Leu) was first identified in a single large consanguineous

family, wherein eight individuals were affected.[7] Subsequently, a small number of cases with other *SLC18A2* variants were reported.[9-12] To date, six disease-causing variants in *SLC18A2* have been reported in seven families, involving 16 affected individuals; among them, only six cases have been described in detail.[7,9-14] In addition, following the first report, each study has described only a single pedigree with one disease-causing variant and thus comprehensive genetic and clinical aspects of the trait remain elusive.

Here, we evaluated 19 homozygous *SLC18A2* variants affecting 42 individuals in 26 families. Together with functional studies, our data could better elucidate the molecular and phenotypic spectra of the VMAT2 aberration.

MATERIALS AND METHODS

Genetic and clinical investigations

We enrolled 42 affected individuals who were newly identified with disease-causing homozygous *SLC18A2* variants through exome/genome sequencing (ES/GS), data sharing with international collaborators and using GeneMatcher.[15] The study was approved by the appropriate Institutional Review Board. Written informed consent to perform genetic studies and publish clinical data, including photographs, was obtained from the parents of all patients. The clinical features of patients were retrospectively

179 investigated.

180 Genomic DNA was isolated from peripheral blood leukocytes using standard
181 procedures, and ES/GS was performed on samples from all affected individuals and in
182 some cases, on samples from their parents. The Genome Aggregation Database
183 (gnomAD)[16] and the UK Biobank database[17] was used to select rare variants that were
184 either absent or present at extremely low frequencies in public databases. NM_003054.6
185 was used as the coding reference sequence for the *SLC18A2* gene. The identified rare
186 disease-causing variants in *SLC18A2* were confirmed using Sanger sequencing of
187 amplicons. The disease causality of variants was evaluated using *in silico* prediction
188 scores.

189

190 **Structural analysis based on homology models**

191 Molecular structural analyses of the mutant proteins were performed based on the
192 conceptual translation of the detected *SLC18A2* variants. Homology models of rat brain
193 vesicular monoamine transporter type 2 (rVMAT2) in the cytoplasm- and lumen-facing
194 conformations (accession numbers PM0078823 and PM0080553, respectively) were
195 obtained from the Protein Model DataBase.[18] A model structure of human VMAT2,
196 predicted using AlphaFold (AF-Q05940-F1-model_v2.pdb), was obtained from the

AlphaFold Protein Structure Database.[19] Structural considerations and figure preparation were performed using PyMOL (Schrodinger, Inc., New York, NY, USA).

SLC18A2 loss-of-function *Caenorhabditis elegans* model

Worm models of genetic diseases are useful for mechanistic studies of disease-related gene function and for drug repurposing screens.[20,21] The treatments for patients with VMAT variants present mixed efficacy, and mutations in the *C. elegans SLC18A2* homolog *cat-1*[22] remain largely uncharacterized. Therefore, we attempted to develop a suitable *C. elegans* model to identify novel candidate treatments *in vivo*. CRISPR-Cas9 was used to generate a large putative LoF mutant, *cat-1*(*syb4974*). Automated quantitative phenotyping was used to evaluate a consistent multidimensional behavioral phenotype of the disease model in comparison with that of the wild-type strain, N2.

Generation of mutant *Caenorhabditis elegans* mutant

The mutant was designed by SunyBiotech using N2 background as a reference. CRISPR guide RNA was designed to target a large deletion (4508 bp), starting close to the start codon and excising several exons from the gene to give high confidence of a putative LoF allele. Deletions were confirmed using polymerase chain reaction.

215

216 **Worm preparation**

217 All strains were cultured on Nematode Growth Medium at 20°C and fed *Escherichia*

218 *coli* (OP50) following a standard procedure.[23] For imaging, synchronized populations of

219 young adult worms were cultured by bleaching unsynchronized gravid adults and

220 allowing L1 diapause progeny to develop for 2.5 days at 20°C (detailed protocol:

221 https://dx.doi.org/10.17504/protocols.io.2bzgap6). On the day of imaging, young adults

222 were washed in M9 (detailed protocol:

223 https://dx.doi.org/10.17504/protocols.io.bfqbjmsn), transferred onto imaging plates (3

224 worms/well) using a COPAS 500 Flow Pilot (detailed protocol:

225 https://dx.doi.org/10.17504/protocols.io.bfc9jiz6), and incubated at 20°C for 3.5 h. The

226 plates were transferred onto a multi-camera tracker for another 30 min for habituation

227 before imaging (detailed protocol: https://dx.doi.org/10.17504/protocols.io.bsicncaw).

228

229 **Image acquisition, processing, and feature extraction.**

230 Videos were acquired and processed following previously described methods.[24] Briefly,

231 videos were acquired in a room with a nominal temperature of 20°C at 25 frames/s at a

232 resolution of 12.4 µm/px. Three videos were recorded sequentially: a 5-min

pre-stimulus video; a 6-min blue-light recording with three 10-s blue light pulses starting at 60, 160, and 260 s; and a 5-min post-stimulus recording.

The videos were segmented and tracked using Tierpsy Tracker.[25] After segmentation and skeletonization, a manual threshold was applied to filter skeletonized objects—likely to be non-worms from feature extraction—that did not meet the following criteria: 200–2000 µm in length and, 20–500 µm in width. In addition, the Tierpsy Tracker viewer was used to mark wells with visible contamination, agar damage, or excess liquid as "bad," and these wells were excluded from further analysis.

Following tracking, we extracted a pre-defined set of 3076 behavioral features for each well in each of the three videos (pre-stimulus, blue light, and post-stimulus).[26] The extraction of behavioral features was performed on a per-track basis, and the features were then averaged across tracks to produce a single feature vector for each well. Significant differences between the pre-stimulus, post-stimulus, and blue-light behavioral feature sets extracted from the LoF mutants compared with the N2 reference strain were calculated using block permutation *t*-tests (https://github.com/Tierpsy/tierpsy-tools-python/blob/master/tierpsytools/analysis/statistical_tests.py). Python (version 3.8.5) was used to perform the analysis using n = 1000000 permutations that were randomly shuffled within, but not between, the

independent days of image acquisition to control for daily variations in the experiments. The *p*-values were then corrected for multiple comparisons using the Benjamini–Hochberg Procedure[27] to control the false discovery rate at 5%.

Pharyngeal pumping assay

Pharyngeal pumps per minute (ppm) of the *C. elegans* strains were determined by counting grinder movements by eye over a 20-s period using a stereomicroscope (detailed protocol: dx.doi.org/10.17504/protocols.io.b3hiqj4e), n = 120 worms. Grinder movements of a single worm were counted three times, and the results were recorded as an average of these values. Significant differences in ppm between the N2 reference strain and *cat-1* (*syb4974*) mutants were calculated using block permutation *t*-tests with n = 10000 permutations.

RESULTS

Genetic and clinical findings in the affected individuals

Four nonsense variants, five frameshift variants, one splice site variant, and nine missense variants (all homozygous) were identified in *SLC18A2* in 27 unrelated families involving 42 affected individuals (**Figure 1a**). Homozygous variants simply facilitated

the establishment of genotype–phenotype correlations. Of the variants identified, 17 were novel, whereas two missense variants (NM_003054.6: c.710C>A p.Pro237His and c.1160C>T p.Pro387Leu) were recurrent, accounting for 43% of the cases (N = 18/42) described herein. The most common recurrent missense variant, p.Pro237His, was identified in 12 affected individuals from six families. This variant had previously been identified in five patients from three families.[9-11] The second most common variant in this cohort was p.Pro387Leu, which was identified in six affected individuals from three families and has also been previously described in different ethnicities. The novel nonsense variant p.Tyr81* was identified in three affected individuals from two unrelated families. All predicted disease-causing *SLC18A2* variants identified in this study were either ultra-rare or absent in multiple population variant databases (**Supplementary Table 1**); however, p.Pro237His was relatively frequent in the general population, and was found in six of 251,386 alleles (0.000024) in gnomAD and 35 of 537,496 alleles (0.000065) in the UK Biobank database as the heterozygous state.[16,17] All nonsense and frameshift variants were expected to result in nonsense-mediated mRNA decay. All missense variants had Phred-scaled Combined Annotation Dependent Depletion scores greater than 25 (**Supplementary Table 1**). Two individuals had other candidate variants; Patient 41 with the homozygous *SLC18A2* variant (c.282delA

287 p.Asp95Thrfs*2) was described previously,[28] and had potentially multiple molecular
288 diagnoses due to compound heterozygous *DDX47* variants (c.[22G>T];[319G>G]
289 p.[p.Asp8Phe];[p.Gln107Glu]) and a homozygous *SLC13A5* variant (c.1444A>G
290 p.Thr482Ala). Patient 39 with the homozygous *SLC18A2* variant (c.282delA
291 p.Asp95Thrfs*2) had another candidate variant in the *TOR1A* gene (c.836T>C
292 p.Met279Thr).

293 Sixteen of the 58 individuals (28 %) described to date (42 individuals in this
294 study and 16 individuals who were previously reported, with homozygous variants) died
295 during childhood (age range: 9 months to 13 years; median: 5.5 years) due to pulmonary
296 complications, sudden cardiorespiratory arrest, or high fever with/without seizures. The
297 clinical features of patients with biallelic disease-causing *SLC18A2* variants detected in
298 the previous and present studies are summarized in **Table 1** and fully described in
299 **Supplementary Table 2**. Except Patient 5, who was prematurely born with a
300 birthweight of 1.3 kg, most affected individuals were neurologically normal at birth
301 with no perinatal problems. A few weeks to a few months after birth, the affected
302 individuals began to manifest muscular hypotonia, feeding difficulties, and global
303 developmental delay. Most individuals presented global developmental delay (100%,
304 57/57), truncal hypotonia (96%, 53/55), dystonia (94%, 51/54), and parkinsonism (73%,

36/49); however, the severity varied. Oculogyric crisis is a critical sign of this genetic disorder (88%, 44/50). Temperature instability or excessive sweating was observed in 71% (32/45) of the patients. Gastrointestinal problems including dysphagia, hypersalivation, and constipation were frequently observed in 63% (32/43), 78% (35/45), and 69% (18/26) of the patients, respectively, and several patients required supplemental nasogastric feeding or gastrostomy. Epilepsy or seizures occurred in 40% (18/45) and other paroxysmal movements were observed in 58% (28/48) of the patients. However, the electroencephalogram (EEG) was normal or at least did not correlate well with seizures or other paroxysmal movements. Several patients showed intentional tremor or ataxia, although we could not obtain sufficient information for most patients.

The brain images were typically normal (40%, 15/37), although subtle changes were occasionally observed (e.g., corpus callosum hypoplasia in 14% [5/37], non-specific white matter abnormalities in 27% [10/37], or cerebral atrophy/cortical volume loss/mild ventricle enlargement in 30% [11/37] of the patients; **Table 1, Supplementary figure 1**). Cerebrospinal fluid (CSF) neurotransmitter analysis was performed in four patients, and homovanillic acid (HVA) and 5-hydroxyindoleacetic acid (5-HIAA) levels were within normal limits (**Supplementary Table 3**).

In total, 80% (33/41) of the patients were non-verbal and most of them were

non-ambulatory. Fourteen affected individuals with nonsense, frameshift, and splice site variants were mostly non-verbal and in a bed-bound state, and had more severe symptoms than those with missense variants (e.g. **Figure 1b**; photographs of Patients 30, 31, 34, 40, and 42 with truncating variants). Notably, differences in disease severity were observed among the affected individuals with missense variants, wherein the patients with p.Pro237His showed severe phenotypes similar to those with null variants, while some with p.Ile43Phe or p.Pro387Leu variants were ambulatory and verbal. Patients 20 and 21, both harboring homozygous p.Ile43Phe variants, started to walk at the age of 3 and 2.5 years, respectively, and speak short sentences at the age of 4 and 3 years, respectively. (**Figure 1b**, **Supplementary Videos e** and **f**). Videos of patients' activity are available for Patients 2, 13–15, 20, 21, 26, 30, 36, and 37 (**Supplementary Materials**).

Levodopa (L-DOPA) treatment was either ineffective or had an adverse effect, whereas dopamine receptor agonist treatment mildly improved symptoms in 81% (17/21) of the patients (**Table 1**, **Supplementary Table 2**). Improvement was observed in alertness, parkinsonism, dystonia, and oculogyric crisis, although it varied with each patient. The dopamine agonist pramipexole at 0.01–0.02 mg/kg/day divided into 1-3 doses was initiated; if a patient tolerated this dose without adverse effects, it was

increased.[29] The increased dose of pramipexole caused agitation or nausea in a few cases.

Mapping of disease-causing *SLC18A2* missense variants on the VMAT2 structural models

The structure of human VMAT2 has not been experimentally determined. However, homology models of the rat protein (rVMAT2) have been constructed using related transporter structures as templates, to represent three conformational states in the transport cycle (cytoplasm-facing, occluded, and lumen-facing conformations).[30,31] These models agree well with a model created by an artificial intelligence-based structure prediction program, AlphaFold2, in terms of distribution of transmembrane helices.[14]

We mapped the positions of missense variants on the structural models of rVMAT2. The models contain two domains (the N- and C-domains), each consisting of six transmembrane helices,[32] and their relative orientation changes between the cytoplasm- and lumen-facing conformations (**Figure 2**). Proline and glycine residues—generally known as "helix breakers"—occur at multiple transmembrane helices and are assumed to facilitate the conformational distortion or flexibility of

359 VMAT2; this is essential for proton-coupled conformational changes in the transport
360 cycle.[32] Notably, among the nine variants reported in this study, four affect prolines
361 (p.Pro42Leu, p.Pro161Arg, p.Pro237His, and p.Pro387Leu) and one affects glycine
362 (p.Gly436Ser) in the transmembrane helices. These variants could perturb the
363 conformational dynamics and subsequently, the transport activity of VMAT2.

364 Specifically, rVMAT2 carrying the p.Pro42Leu substitution (equivalent to
365 human VMAT2 p.Pro42Leu) abolishes serotonin transport activity.[33] In the
366 cytoplasm-facing conformation, Pro42 and the adjacent Ile43 are located at the bottom
367 of the central cavity, which accommodates the monoamine substrates (**Figure 2b**).
368 Pro42 and Ile43 are positioned at the bend of transmembrane helix 1 (TM1) in the
369 cytoplasm-facing conformation (**Figure 2d**); TM1 is stretched in the lumen-facing
370 conformation (**Figure 2c** and **e**). Therefore, the p.Pro42Leu and p.Ile43Phe substitutions
371 may affect this conformational transition of TM1, leading to decreased monoamine
372 transport activity.

373 Similar to Pro42, Ala310 of rVMAT2 (equivalent to human VMAT Ala309)
374 faces the central cavity in the cytoplasm-facing conformation (Figure 2d). It is located
375 on TM7 and is one turn away from Glu313, an essential residue for monoamine
376 transport activity. Glu313 directly binds to the monoamines and/or protons; therefore,

the human p.Ala309Val substitution may affect the transportation. In rVMAT2, Tyr419 (equivalent to human Tyr418) has been proposed to constitute a part of the cytoplasmic gate. The rVMAT2 variants carrying p.Tyr419Ser and p.Tyr419Ala, but not p.Tyr419Phe, lack serotonin transport activities.[31] Therefore, a human VMAT2 variant carrying p.Tyr418Cys, without an aromatic ring, may exhibit impaired transport activity.

Caenorhabditis elegans model mimicking loss-of-function abnormalities in *SLC18A2*

To create a C. elegans disease model we deleted cat-1, the worm homolog of *SLC18A2*. The mutant showed increased curvature of the head and neck and slow movement, and was generally more stationary than the wild type reference strain N2 (**Supplementary Figure 2a–d**). Upon stimulation with an aversive stimulus (pulses of blue light), *cat-1*(*syb4974*) demonstrated a hypersensitive, but short lived, photophobic escape response **(Supplementary Figure 2f–i**). We noted that the *cat-1*(*syb4974*) phenotype closely resembled that of another *C. elegans* model of hypotonia, *nca-2*(*syb1612*), which has a LoF variant in the sodium cation leak channel (unpublished data). Therefore, *C.elegans* exhibits a conserved multi-dimensional behavioral phenotype

based on the variants in different genes; the symptoms overlap with those in humans with the corresponding variant. The observed behavioral phenotypes are noticeable in short recordings with reasonable throughput,[24] making them an appropriate readout for drug repurposing screens similar to others that have been successful in recording *C. elegans* using whole-organism phenotypes.[20,21]

Effects of monoamine on the *C. elegans* model

Consistent with previous reports on the effects of VMAT variants on monoamine-dependent behaviors in *C. elegans*,[34] the *cat-1*(*syb4974*) mutant exhibited a decreased pharyngeal pumping rate when foraging on a bacterial lawn (**Supplementary Figure 2e**). Based on previous studies on the treatment of monoamine disturbances in humans, we exposed the *cat-1*(*syb4974*) worms to carbidopa, dopamine, levodopa, or pramipexole for 4 h. No significant changes were observed in the phenotypes of any *cat-1*(*syb4974*) worms, at any of the concentrations (0.1−500 μM), compared with that of the control worms (exposed to the solvent only) (**Supplementary Figure 3**). The lack of significant modulation by the compounds that we tested may be due to a lack of drug accumulation in the worms[35] and, therefore, longer treatments at higher concentrations should be considered in future studies.

DISCUSSION

Herein, we described the clinical manifestations observed in 42 individuals from 26 families of different ethnicities with 17 novel and 2 previously reported *SLC18A2* variants. Among the affected individuals in the current and previous studies, p.Pro237His is the most common disease-causing variant. This variant is found relatively frequently across multiple variant databases and could be an ancient founder variant. The high mortality rate indicates the poor prognosis of this genetic disorder. Notably, 9 of the 17 patients with p.Pro237His (median age: 5.0 [0.5–14] years) died, whereas all 14 patients with p.Pro387Leu (median age: 11.0 [3–18] years) survived. In addition, although the affected individuals with homozygous *SLC18A2* variants were often in bed-bound states, those with p.Ile43Phe and p.Pro387Leu were able to walk, indicating a mild clinical phenotype. In contrast, the affected individuals with p.Pro237His exhibited a severe phenotype and poor prognosis, similar to those of individuals with truncating variants. Consistent with this observation, Jacobsen *et al*. reported that patients with p.Pro237His showed a more severe phenotype than the individuals with p.Pro387Leu.[9] These observations indicate a phenotype–genotype correlation in *SLC18A2*-related disorder.

Typical patients with *SCL18A2* variants showed global developmental delay, hypotonia, dystonia, parkinsonism, and autonomic nervous system involvement (e.g., temperature dysregulation/sweating, hypersalivation, gastrointestinal dysmotility, and oculogyric dysmotility). Autonomic dysregulation in combination with extrapyramidal movements, in the presence of structurally normal basal ganglia, is an important clinical feature to distinguish cerebral palsy from this neurotransmitter disease. Other neurotransmitter disorders, such as *SLC6A3*-related DATS and aromatic l-amino acid decarboxylase (AADC) deficiency (MIM# 608643),[36] are possible differential diagnoses, and CSF neurotransmitter analyses are essential diagnostic tests. Typically, *SLC6A3*-related DATS have a high HVA with a normal 5-HIAA ratio (CSF HVA:5-HIAA ratio >5), whereas AADC deficiency has low levels of both HVA and 5-HIAA.[5,36] In contrast, both HVA and 5-HIAA levels in the CSF were within the normal limits in this *SLC18*-related disorder, which is a key finding differentiating other neurotransmitter disorders. These observations are consistent with previous reports.[7,9,12]

Both p.Pro237His and p.Pro387Leu variants affect proline residues located on transmembrane helices (**Figure 2a, b**), and patients with p.Pro237His have severe phenotypes. In the cytoplasm- and lumen-facing conformation of rVMAT2 (**Figure 2c** and **e**), Pro238 (equivalent to human VMAT2 Pro237) is located at the interface

449 between the N- and C-domains, presumably forming a part of the “hinge” region in the
450 conformation of the two domains. Therefore, the Pro237His substitution in human
451 VMAT2 could also affect the conformations of the two domains during the transport
452 cycle. Alternatively, the Pro237His variant could be energetically unstable because of
453 the relatively hydrophilic Pro237His side-chain embedded in the lipid bilayer.
454 VMAT2 is well established as a therapeutic target.[29,37] Notably, L-DOPA is
455 either ineffective or worsens the symptoms in patients, whereas dopamine receptor
456 agonists improve the symptoms. The treatment efficacy was difficult to assess due to
457 the short treatment periods; however, a mild symptom improvement was observed in
458 81% of the patients treated with a dopamine receptor. This finding is inconsistent with
459 the earliest report describing a dramatic therapeutic effect of a dopamine receptor
460 agonist in a large family of patients with p.Pro387Leu variants.[7] p.Pro387Leu causes a
461 relatively mild phenotype, and drug responses should be cautiously evaluated alongside
462 phenotype−genotype correlation.[9] Patients 20 and 21 from Family 11 (with p.Ile43Phe)
463 were able to walk and speak, even without treatment; therefore, certain genetic variants
464 may have a higher effect on illness severity than the treatment itself.
465 A *C. elegans* model was constructed to mimic the affected individuals with
466 LoF variants; it exhibited slow movement, a hypersensitive but short-lived photophobic

escape response, and a decreased pharyngeal pumping rate. Therefore, the *SLC18A2* LoF could be harmful, at least in worms and humans. We did not observe any rescue of *cat-1* mutant phenotypes in response to dopamine or dopamine agonists at the tested concentrations.

The solute carrier (SLC) protein family is a superfamily of transmembrane transporters with over 400 members that are involved in the exchange of amino acids, nutrients, ions, metals, neurotransmitters, and metabolites across various biological membranes.[38] To date, 287 SLC genes have been found in the brain, and mutations or dysfunctions of over 70 SLC-encoding genes have been shown to be associated with a variety of human brain disorders, such as severe developmental delay or epileptic encephalopathies.[39-42]

In summary, in combination with previously published data, we identified the genetic and clinical features of 42 newly affected individuals with homozygous *SLC18A2* variants. We elucidated the clinical synopsis of the trait together with functional study results. These findings may facilitate the establishment of genotype–phenotype correlations for *SLC18A2*-associated parkinsonism-dystonia syndrome. This allelic series study provides initial insights into *SLC18A2*-related disorders with both diagnostic and therapeutic implications.

485

486 **FIGURE LEGENDS**

487 **Figure 1. (a)** Familial pedigrees of 26 families consisting of 42 affected individuals

488 with homozygous solute carrier family 18 member A2 gene (*SLC18A2*) variants. **(b)**

489 Clinical photographs of patients 2, 4–6, 13–16, 19–24, 27, 28, 30, 31, 34, 40, and 42.

490

491 **Figure 2.** Protein structures in two **(a)** and three **(b–d)** dimensions. The positions of the

492 disease-causing variants are mapped onto the homology models of rat vesicular

493 monoamine transporter type 2 (rVMAT2). The N- and C- domains are colored green

494 and cyan, respectively. The rat residues and corresponding human disease-causing

495 variants (in parentheses) are indicated. The central cavity, which accommodates

496 substrates in the cytoplasm-facing conformation is indicated using a red dotted line. **(b,**

497 **c)**, Cytoplasm-facing **(b)** and lumen-facing **(c)** conformations. Left, side view. Right,

498 top view from the cytoplasm. **(d, e)** The structures of transmembrane helix 1 (TM1) and

499 TM7 in the cytoplasm-facing **(d)** and lumen-facing **(e)** conformations.

500

501 **WEB RESOURCES used for this study**

502 AlphaFold Protein Structure Database: https://alphafold.ebi.ac.uk

Combined Annotation Dependent Depletion (CADD):

https://cadd.gs.washington.edu/snv

dbSNP: http://www.ncbi.nlm.nih.gov/snp

Genome Aggregation Database (gnomAD): http://gnomad.broadinstitute.org/

Human Gene Mutation Database (HGMD®) professional 2022.2:

http://portal.biobase-international.com/hgmd

MutationTaster: http://www.mutationtaster.org/

Online Mendelian Inheritance in Man (OMIM®): https://www.omim.org/

PolyPhen-2: http://genetics.bwh.harvard.edu/pph2/

Protein Model DataBase: http://srv00.recas.ba.infn.it/PMDB/

Sorting Intolerant From Tolerant (SIFT): http://sift.jcvi.org

SLC TABLES: http://slc.bioparadigms.org/

Tierpsy: https://tierpsy.com/code

UCSC Genome Browser: http://genome.ucsc.edu/

DATA AVAILABITITY

The datasets of this study are not publicly available due to concerns regarding patients' anonymity. We will supply de-identified data upon request.

ACKNOWLEDGEMENTS

We thank the participants and their families for their involvement in this study.

FUNDING

This work was supported by the Japan Agency for Medical Research and Development (AMED) under grant numbers JP22ek0109486, JP22ek0109549, and JP22ek0109493 (N. Ma.); JSPS KAKENHI under grant numbers JP19H03621 (N. Mi.), JP20K07907 (S. M.), JP20K08164 (T. Miz.), JP20K17936 (A. F.), JP20K16932 (K. H.), and JP21k15907 (Y. U.); and the Takeda Science Foundation (T. M., N. Mi. and N. Ma.). This study was partially supported by the U.S. National Human Genome Research Institute (NHGRI) and National Heart Lung and Blood Institute (NHBLI) to the Baylor-Hopkins Center for Mendelian Genomics (BHCMG, UM1 HG006542 to J.R.L.); U.S. National Institute of Neurological Disorders and Stroke (NINDS, R35NS105078 to J.R.L.) and Muscular Dystrophy Association (MDA, 512848 to J.R.L.). D.Ma. was supported by a Medical Genetics Research Fellowship Program through the National Institutes of Health (NIH, T32 GM007526-42). D.P. was supported by a Clinical Research Training Scholarship in Neuromuscular Disease partnered by the American Academy of Neurology (AAN), American Brain Foundation (ABF), and Muscle Study Group (MSG), and by the International Rett Syndrome Foundation (IRSF, grant number #3701-1). J.E.P. was supported by the NHGRI (K08 HG008986). H.H. was funded by the MRC (MR/S01165X/1, MR/S005021/1, and G0601943), National Institute for Health Research University College London Hospitals Biomedical Research Centre, Rosetree Trust, Ataxia UK, Multiple System Atrophy Trust, Brain Research UK, Sparks Great Ormond Street Hospital Charity, Muscular Dystrophy UK (MDUK), and Muscular Dystrophy Association USA. S.E. was supported by an MRC strategic award to establish an International Centre for Genomic Medicine in Neuromuscular Diseases (ICGNMD, MR/S005021/1). This project also received funding from the European Research Council (ERC) under the European Union's Horizon 2020 Research and Innovation Program (Grant Agreement No. 714853) and was supported by the Medical Research Council through grant MC-A658-5TY30. We acknowledge the support of King Salman Center for Disability Research through Research Group no RG-2022-010 (F.S.A.).

Author Contributions: K.Sai. and R.M. conceived and designed the study, interpreted the data and wrote the manuscript. T.S. and K.O. conducted protein structure analysis

and wrote the manuscript. T.J.O. and E.G.K. performed the *C. elegans* experiments. T.Mit., M.T., H.Y.L., G.A., H.G., M.Z., M.B.T., F.As., S.I., H.M., N.A., V.K.G., V.M.S., D.Ma., R.K., N.D., H.T., H.M.E., K.R., S.Y., S.K., M.H., M.P., D.A., J.R.M.C., C.A.K., K.G.M., K.G.L., H.Y., M.S.Z., R.M.E., K.Sal., U.G., M.M., S.S., and M.A. recruited the patients and performed the clinical evaluation. D.P., M.Se., M.Sr., D.B., S.Als., S.Ala., S.A.M.M., H.A., M.A.O., L.A., F.Ab., T.J., R.E.G., H.S., D.K., T.S.R., F.S., D.Mi and B.A. helped obtain clinical information on the patients reported in this study. A.T.P., Y.B., A.M., G.Y., E.S., S.G., and D.P. contributed to genetic data analysis. S.O., K.H., A.F., Y.U., T.Miz., S.M., E.F., D.Mu., R.R., and C.J.C. conducted DNA sequencing and genetic data analysis. P.S., A.G., F.S.A., A.E.B., and J.E.P. evaluated the data and wrote the manuscript. N.Mi., J.G.G., J.R.L., H.H., and N.Ma. conducted and supervised this study, wrote the manuscript, and secured funding.

ETHICS DECLARATION: Written informed consent for publication was obtained from the parents of each patient. Ethics approval for this study was obtained from the Institutional Review Board of Yokohama City University School of Medicine, Baylor College of Medicine, University College London, the Norwegian South-Eastern Regional Ethics Committee, and each genetic analysis center.

REFERENCES

1. Ng J, Papandreou A, Heales SJ, Kurian MA. Monoamine neurotransmitter disorders--clinical advances and future perspectives. Nat Rev Neurol. 2015;11(10):567-584.
2. Blackstone C. Infantile parkinsonism-dystonia: a dopamine "transportopathy". J Clin Invest. 2009;119(6):1455-1458.
3. Kurian MA, Gissen P, Smith M, Heales S, Jr., Clayton PT. The monoamine neurotransmitter disorders: an expanding range of neurological syndromes. Lancet Neurol. 2011;10(8):721-733.
4. Kurian MA, Zhen J, Cheng SY, et al. Homozygous loss-of-function mutations in the gene encoding the dopamine transporter are associated with infantile parkinsonism-dystonia. J Clin Invest. 2009;119(6):1595-1603.
5. Kurian MA. SLC6A3-Related Dopamine Transporter Deficiency Syndrome. In: Adam MP, Mirzaa GM, Pagon RA, et al., editors. GeneReviews((R)). Seattle (WA)1993.
6. Fon EA, Pothos EN, Sun BC, Killeen N, Sulzer D, Edwards RH. Vesicular

transport regulates monoamine storage and release but is not essential for amphetamine action. Neuron. 1997;19(6):1271-1283.
7. Rilstone JJ, Alkhater RA, Minassian BA. Brain dopamine-serotonin vesicular transport disease and its treatment. N Engl J Med. 2013;368(6):543-550.
8. Takahashi N, Miner LL, Sora I, et al. VMAT2 knockout mice: heterozygotes display reduced amphetamine-conditioned reward, enhanced amphetamine locomotion, and enhanced MPTP toxicity. Proc Natl Acad Sci U S A. 1997;94(18):9938-9943.
9. Jacobsen JC, Wilson C, Cunningham V, et al. Brain dopamine-serotonin vesicular transport disease presenting as a severe infantile hypotonic parkinsonian disorder. J Inherit Metab Dis. 2016;39(2):305-308.
10. Zhai H, Zheng Y, He Y, et al. A case report of infantile parkinsonism-dystonia-2 caused by homozygous mutation in the SLC18A2 gene. Int J Neurosci. 2021:1-4.
11. Rath M, Korenke GC, Najm J, et al. Exome sequencing results in identification and treatment of brain dopamine-serotonin vesicular transport disease. J Neurol Sci. 2017;379:296-297.
12. Padmakumar M, Jaeken J, Ramaekers V, et al. A novel missense variant in SLC18A2 causes recessive brain monoamine vesicular transport disease and absent serotonin in platelets. JIMD Rep. 2019;47(1):9-16.
13. Ziats MN, Ahmad A, Bernat JA, et al. Genotype-phenotype analysis of 523 patients by genetics evaluation and clinical exome sequencing. Pediatr Res. 2020;87(4):735-739.
14. Patel N, Khan AO, Alsahli S, et al. Genetic investigation of 93 families with microphthalmia or posterior microphthalmos. Clin Genet. 2018;93(6):1210-1222.
15. Sobreira N, Schiettecatte F, Valle D, Hamosh A. GeneMatcher: a matching tool for connecting investigators with an interest in the same gene. Hum Mutat. 2015;36(10):928-930.
16. Karczewski KJ, Francioli LC, Tiao G, et al. The mutational constraint spectrum quantified from variation in 141,456 humans. Nature. 2020;581(7809):434-443.
17. Bycroft C, Freeman C, Petkova D, et al. The UK Biobank resource with deep phenotyping and genomic data. Nature. 2018;562(7726):203-209.
18. Castrignano T, De Meo PD, Cozzetto D, Talamo IG, Tramontano A. The PMDB Protein Model Database. Nucleic Acids Res. 2006;34(Database issue):D306-309.

19. Tunyasuvunakool K, Adler J, Wu Z, et al. Highly accurate protein structure prediction for the human proteome. Nature. 2021;596(7873):590-596.
20. Iyer S, Sam FS, DiPrimio N, et al. Repurposing the aldose reductase inhibitor and diabetic neuropathy drug epalrestat for the congenital disorder of glycosylation PMM2-CDG. Dis Model Mech. 2019;12(11).
21. Patten SA, Aggad D, Martinez J, et al. Neuroleptics as therapeutic compounds stabilizing neuromuscular transmission in amyotrophic lateral sclerosis. JCI Insight. 2017;2(22).
22. Sato DX, Kawata M. Positive and balancing selection on SLC18A1 gene associated with psychiatric disorders and human-unique personality traits. Evol Lett. 2018;2(5):499-510.
23. Stiernagle T. Maintenance of C. elegans. WormBook. 2006:1-11.
24. Barlow IL, Feriani L, Minga E, et al. Megapixel camera arrays enable high-resolution animal tracking in multiwell plates. Commun Biol. 2022;5(1):253.
25. Javer A, Currie M, Lee CW, et al. An open-source platform for analyzing and sharing worm-behavior data. Nat Methods. 2018;15(9):645-646.
26. Javer A, Ripoll-Sanchez L, Brown AEX. Powerful and interpretable behavioural features for quantitative phenotyping of Caenorhabditis elegans. Philos Trans R Soc Lond B Biol Sci. 2018;373(1758).
27. Benjamini Y, Drai D, Elmer G, Kafkafi N, Golani I. Controlling the false discovery rate in behavior genetics research. Behav Brain Res. 2001;125(1-2):279-284.
28. Paine I, Posey JE, Grochowski CM, et al. Paralog Studies Augment Gene Discovery: DDX and DHX Genes. Am J Hum Genet. 2019;105(2):302-316.
29. Ng J, Heales SJ, Kurian MA. Clinical features and pharmacotherapy of childhood monoamine neurotransmitter disorders. Paediatr Drugs. 2014;16(4):275-291.
30. Yaffe D, Radestock S, Shuster Y, Forrest LR, Schuldiner S. Identification of molecular hinge points mediating alternating access in the vesicular monoamine transporter VMAT2. Proc Natl Acad Sci U S A. 2013;110(15):E1332-1341.
31. Yaffe D, Vergara-Jaque A, Forrest LR, Schuldiner S. Emulating proton-induced conformational changes in the vesicular monoamine transporter VMAT2 by mutagenesis. Proc Natl Acad Sci U S A. 2016;113(47):E7390-E7398.
32. Yaffe D, Forrest LR, Schuldiner S. The ins and outs of vesicular monoamine transporters. J Gen Physiol. 2018;150(5):671-682.

33. Ugolev Y, Segal T, Yaffe D, Gros Y, Schuldiner S. Identification of conformationally sensitive residues essential for inhibition of vesicular monoamine transport by the noncompetitive inhibitor tetrabenazine. J Biol Chem. 2013;288(45):32160-32171.
34. Duerr JS, Frisby DL, Gaskin J, et al. The cat-1 gene of Caenorhabditis elegans encodes a vesicular monoamine transporter required for specific monoamine-dependent behaviors. J Neurosci. 1999;19(1):72-84.
35. Burns AR, Wallace IM, Wildenhain J, et al. A predictive model for drug bioaccumulation and bioactivity in Caenorhabditis elegans. Nat Chem Biol. 2010;6(7):549-557.
36. Wassenberg T, Molero-Luis M, Jeltsch K, et al. Consensus guideline for the diagnosis and treatment of aromatic l-amino acid decarboxylase (AADC) deficiency. Orphanet J Rare Dis. 2017;12(1):12.
37. Kurian MA, Li Y, Zhen J, et al. Clinical and molecular characterisation of hereditary dopamine transporter deficiency syndrome: an observational cohort and experimental study. Lancet Neurol. 2011;10(1):54-62.
38. Zhang Y, Zhang Y, Sun K, Meng Z, Chen L. The SLC transporter in nutrient and metabolic sensing, regulation, and drug development. J Mol Cell Biol. 2019;11(1):1-13.
39. Duan R, Saadi NW, Grochowski CM, et al. A novel homozygous SLC13A5 whole-gene deletion generated by Alu/Alu-mediated rearrangement in an Iraqi family with epileptic encephalopathy. Am J Med Genet A. 2021;185(7):1972-1980.
40. Marafi D, Fatih JM, Kaiyrzhanov R, et al. Biallelic variants in SLC38A3 encoding a glutamine transporter cause epileptic encephalopathy. Brain. 2022;145(3):909-924.
41. Saitsu H, Watanabe M, Akita T, et al. Impaired neuronal KCC2 function by biallelic SLC12A5 mutations in migrating focal seizures and severe developmental delay. Sci Rep. 2016;6:30072.
42. Hu C, Tao L, Cao X, Chen L. The solute carrier transporters and the brain: Physiological and pharmacological implications. Asian J Pharm Sci. 2020;15(2):131-144.

Figure 1

a

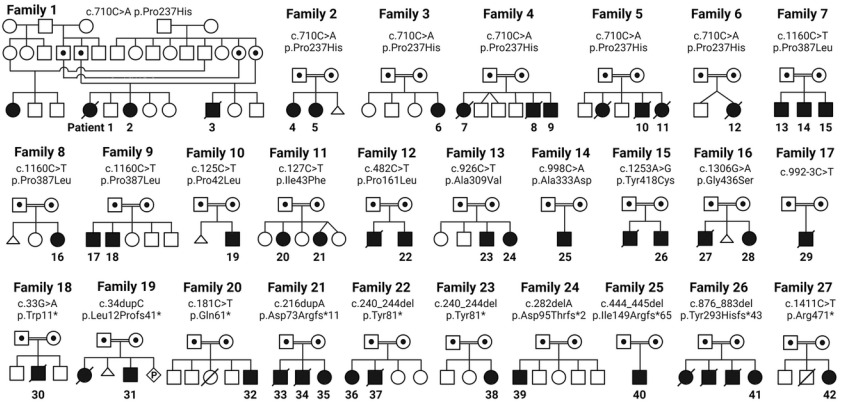
Family 1
c.710C>A p.Pro237His
Patient 1
1
2
3
Family 2
c.710C>A
p.Pro237His
4
5
Family 3
c.710C>A
p.Pro237His
6
Family 4
c.710C>A
p.Pro237His
7
8
9
Family 5
c.710C>A
p.Pro237His
10
11
Family 6
c.710C>A
p.Pro237His
12
Family 7
c.1160C>T
p.Pro387Leu
13
14
15
Family 8
c.1160C>T
p.Pro387Leu
16
Family 9
c.1160C>T
p.Pro387Leu
17
18
Family 10
c.125C>T
p.Pro42Leu
19
Family 11
c.127C>T
p.Ile43Phe
20
21
Family 12
c.482C>T
p.Pro161Leu
22
Family 13
c.926C>T
p.Ala309Val
23
24
Family 14
c.998C>A
p.Ala333Asp
25
Family 15
c.1253A>G
p.Tyr418Cys
26
Family 16
c.1306G>A
p.Gly436Ser
27
28
Family 17
c.992-3C>T
29
Family 18
c.33G>A
p.Trp11*
30
Family 19
c.34dupC
p.Leu12Profs41*
31
Family 20
c.181C>T
p.Gln61*
32
Family 21
c.216dupA
p.Asp73Argfs*11
33
34
35
Family 22
c.240_244del
p.Tyr81*
36
37
Family 23
c.240_244del
p.Tyr81*
38
Family 24
c.282delA
p.Asp95Thrfs*2
39
Family 25
c.444_445del
p.Ile149Argfs*65
40
Family 26
c.876_883del
p.Tyr293Hisfs*43
41
Family 27
c.1411C>T
p.Arg471*
42

b


Patient 2
p.Pro237His
Patient 4, 5
p.Pro237His
Patient 6
p.Pro237His
Patient 13-15
p.Pro387Leu
Patient 16
p.Pro387Leu
Patient 19
p.Pro42Leu
Patient 20, 21
p.Ile43Phe
Patient 23, 24
p.Ala309Val
Patient 27, 28
p.Gly436Ser
Patient 30
p.Trp11*
Patient 31
p.Leu12Profs*41
Patient 34
p.Tyr81*
Patient 40
p.Ile149Argfs*65
Patient 42
p.Arg471*

Figure 2

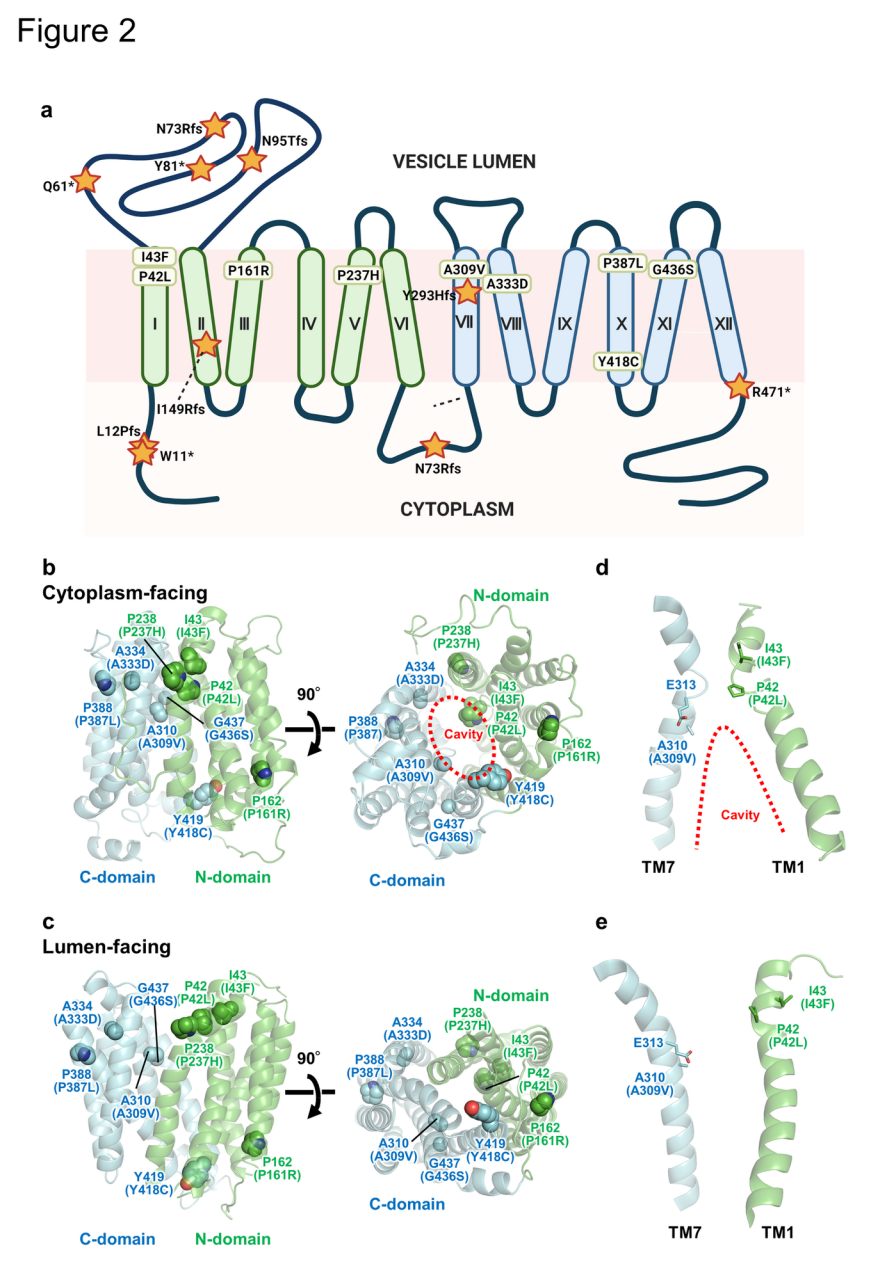
a
N73Rfs
N95Tfs
Y81*
Q61*
VESICLE LUMEN
I43F
P42L
P161R
P237H
A309V
A333D
Y293Hfs
P387L
G436S
I
II
III
IV
V
VI
VII
VIII
IX
X
XI
XII
Y418C
R471*
I149Rfs
L12Pfs
W11*
N73Rfs
CYTOPLASM
b
Cytoplasm-facing
P238 (P237H)
I43 (I43F)
A334 (A333D)
P42 (P42L)
P388 (P387L)
G437 (G436S)
A310 (A309V)
P162 (P161R)
Y419 (Y418C)
C-domain
N-domain
90˚
N-domain
P238 (P237H)
A334 (A333D)
I43 (I43F)
P42 (P42L)
Cavity
P388 (P387)
P162 (P161R)
A310 (A309V)
Y419 (Y418C)
G437 (G436S)
C-domain
c
Lumen-facing
G437 (G436S)
P42 (P42L)
I43 (I43F)
A334 (A333D)
P238 (P237H)
P388 (P387L)
A310 (A309V)
Y419 (Y418C)
P162 (P161R)
C-domain
N-domain
90˚
N-domain
A334 (A333D)
P238 (P237H)
I43 (I43F)
P388 (P387L)
P42 (P42L)
P162 (P161R)
A310 (A309V)
Y419 (Y418C)
G437 (G436S)
C-domain
d
E313
I43 (I43F)
P42 (P42L)
A310 (A309V)
Cavity
TM7
TM1
e
E313
I43 (I43F)
P42 (P42L)
A310 (A309V)
TM7
TM1

		Missense Variants			Truncating and splice site variants	Total
		Recurrent variant p.Pro237His	Recurrent variant p.Pro387Leu	Other missense variants		
Demographic	Number of patients	*n* = 17	*n* = 14	*n* = 11	*n* = 15	*n* = 57*
	Gender (Male/Female)	8 M/ 9 F	10 M/ 4 F	6 M/ 5 F	8 M/ 7 F	32 M/ 25 F
	Mortality (Living status)	53% 8 living/ 9 dead	0% 14 living/ 0 dead	18% 9 living/ 2 dead	33% 10 living/ 5 dead	28% 41 living/ 16 dead
	Age range (median)	5.0 years [0.5–14]	11.0 years [3–18]	6.3 years [1–25]	6.0 years [2–16]	5.5 years [0.5–25]
Clinical features	GDD/ID	17/17	14/14	11/11	15/15	100% (57/57)
	Truncal hypotonia	17/17	14/14	9/11	13/13	96% (53/55)
	Dystonia	16/16	12/14	10/10	13/14	94% (51/54)
	Parkinsonism	12/16	11/14	6/9	7/10	73% (36/49)
	Non-verbal	13/15	4/7	7/9	9/10	80% (33/41)
	Oculogyric crises	12/12	12/14	9/10	12/14	88% (44/50)
	Epilepsy/Seizures	7/12	2/11	5/10	4/12	40% (18/45)
	Other paroxysmal movements	8/14	9/11	4/10	7/13	58% (28/48)
	Temperature instability/sweating	10/12	8/14	6/8	8/11	71% (32/45)
	Feeding issues (Dysphagia/NG tube/gastrostomy)	8/14	3/7	6/10	10/12	63% (32/43)
	Hypersalivation (Drooling)	10/11	12/14	5/9	8/11	78% (35/45)
	Constipation	3/4	1/2	5/7	9/12	69% (18/26)
Imaging findings	Normal findings	8/15	2/5	3/7	2/10	40% (15/37)
	Corpus callosum hypoplasia	1/15	0/5	1/7	3/10	14% (5/37)
	Non-specific WM abnormalities	2/15	2/5	1/7	5/10	27% (10/37)
	Brain atrophy	4/15	1/5	2/7	4/10	30% (11/37)
Treatment	L-DOPA use	3/18	4/14	8/11	5/14	35% (20/57)
	Deterioration on L-DOPA	3/3	4/4	2/8	3/5	60% (12/20)
	Dopamine receptor agonist use	3/18	5/14	7/11	6/14	37% (21/57)
	Improvement on dopamine agonist	3/3	5/5	6/7	4/6	86% (18/21)

Table 1. Summary of the clinical features of all patients (current and previously reported) with disease-causing biallelic *SLC18A2* variants

*A patient with compound heterozygous variants (c.[895G>C];[835_836delAG] p.[Gly299Arg];[Gln280Glufs*58]) (PMID: 31618753) was excluded from Table 1 because of a lack of detailed clinical information.

LoF, loss-of-function; GDD, Global developmental delay; ID, Intellectual disability; NG, nasogastric; WM, white matter; L-DOPA, levodopa

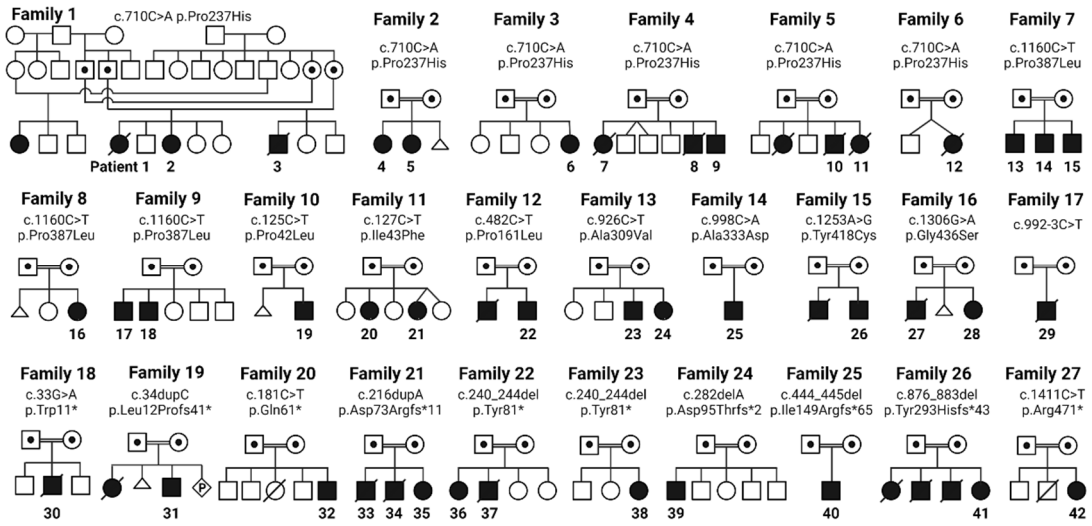

A global cohort identified 42 patients from 27 families with brain monoamine vesicular transport disease arising from homozygous *SLC18A2* variants.